Magazine of Concrete Research
Volume 66 Issue 18

A micromechanical model for concrete under static loading
Teng, Li and Liu

Magazine of Concrete Research, 2014, **66**(18), 913–924
http://dx.doi.org/10.1680/macr.14.00024
Paper 1400024
Received 22/01/2014; revised 13/03/2014; accepted 14/03/2014
Published online ahead of print 20/05/2014

A micromechanical model for concrete under static loading

Susanto Teng
Associate Professor, School of Civil and Environmental Engineering (CEE), Nanyang Technological University (NTU), Singapore

Qingliu Li
Structural Engineer, Singapore Technologies Engineering, Singapore

Yu Liu
Senior Research Fellow, CEE, NTU, Singapore

A micromechanical model is developed to describe the stress–strain behaviours of concrete under uniaxial compression. Two kinds of defects are considered, namely microcracks around the mortar–coarse aggregate interface or the interfacial transition zone and aligned coalesced cracks in the concrete. The mortar–coarse aggregate interfaces (interfacial transition zone) are modelled as spring layers between the mortar matrix and the inclusions (aggregates) and the existences of the microcracks in the interfacial transition zone are considered as reductions of the spring parameters under the frame of the Mori–Tanaka method. The aligned coalesced cracks in concrete (mortar + aggregate) are treated as void inclusions in the matrix of concrete using the Mori–Tanaka scheme as well. Stochastic evolution rules are adopted for both defects. The numerical examples are worked out and the proposed model is shown to be capable of estimating the moduli of concrete under its whole loading process.

Notation

A_0	constants in Eshelby's tensor
a	average radius of coarse aggregates
B_0	constants in Eshelby's tensor
c_1, c_2	volume fractions of mortar and aggregate
c_i	fraction of failed interfaces
c_v	volume ratio of aligned cracks to overall concrete
E_e	Young's modulus of the concrete with imperfect interfaces
E_0, E_1	Young's moduli of mortar and coarse aggregate
$\boldsymbol{e}$	deviatoric strain tensor
f'_c	compressive strength for concrete
f_t	tensile strength for concrete
G_F	fracture energy of concrete
g	aggregate size
$\boldsymbol{I}$	identity tensor
k_1, k_2, k_3, k_4	constants in Eshelby's tensor
$\boldsymbol{L}_0$	elastic stiffnesses of mortar
$\boldsymbol{L}_1$	elastic stiffnesses of coarse aggregates
l_m	Eigen-length for mortar
m_1	shape factor in fraction of failed interfaces ($=3$)
m_2	shape factor in volume ratio of aligned cracks to overall concrete
N	normal traction
$\boldsymbol{n}$	external normal of representative volume element
S	external surface of representative volume element
$\boldsymbol{S}^E_{ijkl}$	Eshelby's tensor for perfectly bonded interface
S^S_{ijkl}	additional term in Eshelby's tensor considering imperfect interface
$\boldsymbol{s}$	deviatoric stress tensor
$\boldsymbol{T}$	shear traction
u^S_i	displacement fields caused by the interfacial sliding and normal separation
V	volume of representative volume element
w	density of concrete
α^0, α^E, α^S	constants in Eshelby's tensor
α_F	coefficient related to the fracture energy of concrete
α_T, α_N	tangential and normal compliance of mortar–coarse aggregate interface
β^0, β^E, β^S	constants in Eshelby's tensor
β_F	coefficient related to the eigen-length for mortar ($=0.5$)
ε	hydrostatic strain
$\tilde{\boldsymbol{\varepsilon}}$	perturbed strains due to the presence of coarse aggregates
$\boldsymbol{\varepsilon}^*$	equivalent transformation strains
$\boldsymbol{\varepsilon}^0$	far field constant strain tensor
$\varepsilon_\mathrm{lateral}$, $\bar{\varepsilon}_\mathrm{lateral}$	lateral strain and modified lateral strain of concrete
$\boldsymbol{\varepsilon}^\mathrm{pt}$	further perturbed strains in coarse aggregates
ε_r	parameter related to the shape factor M_2
$\boldsymbol{\varepsilon}^\mathrm{S}$	strain caused by the interfacial sliding and normal separation
ε_u1	ultimate compressive strain ($=0{\cdot}008$)
ε_u2	ultimate tensile strain value
δ_{ij}	Kronecker delta
κ	equivalent bulk modulus of concrete
κ_0, κ_1	bulk moduli of mortar and coarse aggregates
κ_d, κ_p	bulk moduli of concrete with destroyed and perfect interface

λ_0	constants in Eshelby's tensor
λ_l	constants in modified lateral strain of concrete
μ	equivalent shear modulus of concrete
μ_0, μ_1	shear moduli of mortar and coarse aggregate
μ_d, μ_p	shear moduli of concrete with destroyed and perfect interface
υ_0	Poisson ratio of mortar matrix
υ_e	Poisson ratio of the concrete with imperfect interfaces
ρ_0, ρ_1	densities of mortar and coarse aggregate
σ	hydrostatic stress
$\bar{\boldsymbol{\sigma}}$	overall average stress tensor
$\tilde{\boldsymbol{\sigma}}$	perturbed stresses due to the presence of coarse aggregates
$\boldsymbol{\sigma}^0$	far field constant stress tensor
$\boldsymbol{\sigma}^{(0)}$, $\boldsymbol{\sigma}^{(1)}$	average stress in mortar and coarse aggregates
$\boldsymbol{\sigma}^{pt}$	further perturbed stresses in coarse aggregates
Ω, $\partial\Omega$	spherical inclusion and its interface

Introduction

Constitutive models for concrete are needed in the numerical analysis of concrete structures. Usually, the behaviour of concrete can be modelled at different scales, which leads to three categories of models: macroscopic level models, mesoscopic level models and microscopic level models. The macroscopic level models, such as elasto-plastic models, fracturing models and continuum damage models, have been widely used in the practice of structural analysis. Meanwhile, the mesoscopic and microscopic level models, such as particle simulation models, microplane models and models based on equivalent modulus method have shown their advantages when studying the failure mechanism of materials. Models based on the equivalent modulus method especially, seem to be a natural choice because they model the concrete as a composite made of mortar and aggregates. A number of researchers have studied the elastic properties of concrete using equivalent modulus methods, such as the self-consistent method (Hashin and Monteiro, 2002; Ramesh *et al.*, 1996), the Mori–Tanaka method (Ricaud and Masson, 2009; Yang and Huang, 1996), and numerical methods such as discrete element model (He *et al.*, 2012; Zheng *et al.*, 2011).

In this paper, a micromechanical model based on the Mori–Tanaka method (Benveniste, 1987; Mori and Tanaka, 1973) is proposed. The concrete is considered as a two-phase composite (mortar + coarse aggregates). Some experiments (Nilsen and Monteiro, 1993) have shown that the matrix just surrounding the aggregate, the so-called interfacial transition zone (ITZ) is found to have quite different stiffness properties than that further away from the aggregate, since there are many microcracks in this zone even before any loading is applied. The ITZ is thus modelled as a spring layer including a normal spring and a tangential spring, as shown in Figure 1. The degradation of the mortar–coarse aggregate interfaces is modelled as the progressive failure of the spring layers. Figure 2(a) shows a two-phase composite with zero-thickness ITZ. With degradation of the ITZ, the moduli of concrete reduced and it is assumed to be homogeneous, as shown in Figure 2(b). Other cracks in the concrete are assumed to coalesce and align perpendicularly with respect to the principal tensile strain. These are modelled as ellipsoidal void inclusions in the matrix of the concrete (mortar + coarse aggregate) also under the frame of the Mori–Tanaka method, as shown in Figure 2(c).

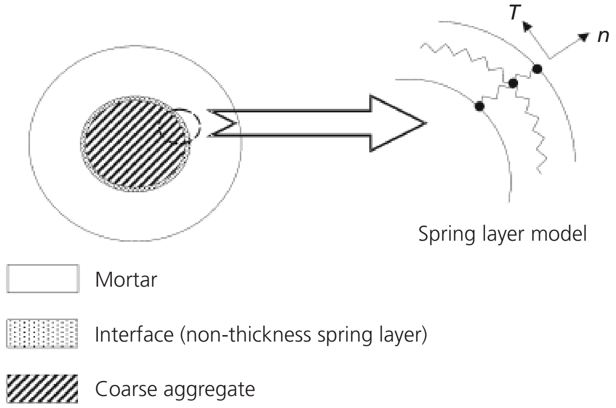

Figure 1. Two-phase model with imperfect interface

To obtain the full stress–strain curves, the evolution rules for these defects or damage are needed. In this paper, stochastic evolution rules are adopted for both kinds of defects, namely the increase of failure of mortar–coarse aggregate interfaces and the volume ratio of aligned coalesced cracks in the concrete are all assumed to follow a Weibull distribution with separate parameters.

Equivalent moduli of concrete with imperfect ITZ

When load is applied to concrete, microcracks around the mortar–course aggregate interfaces are first observed. In this paper, the interfaces are considered as a zero-thickness spring layer under the frame of the Mori–Tanaka method (Figure 1).

Basic formulation

Consider an infinitely extended mortar medium D containing many spherical inclusions (coarse aggregates) with an imperfectly bonded interface under the frame of the Mori–Tanaka method. The elastic stiffnesses of the mortar and the coarse aggregates are $\boldsymbol{L}_0$ and $\boldsymbol{L}_1$, respectively. A homogeneous boundary condition on the external surface S is assumed, thus

$$1.\quad \boldsymbol{\sigma}_n(S) = \boldsymbol{\sigma}^0\boldsymbol{n}$$

where $\boldsymbol{\sigma}^0$ is the constant stress tensor, and $\boldsymbol{n}$ is the external normal to the external surface $\boldsymbol{S}$. If the mortar did not contain any inhomogeneity, the strain field would be

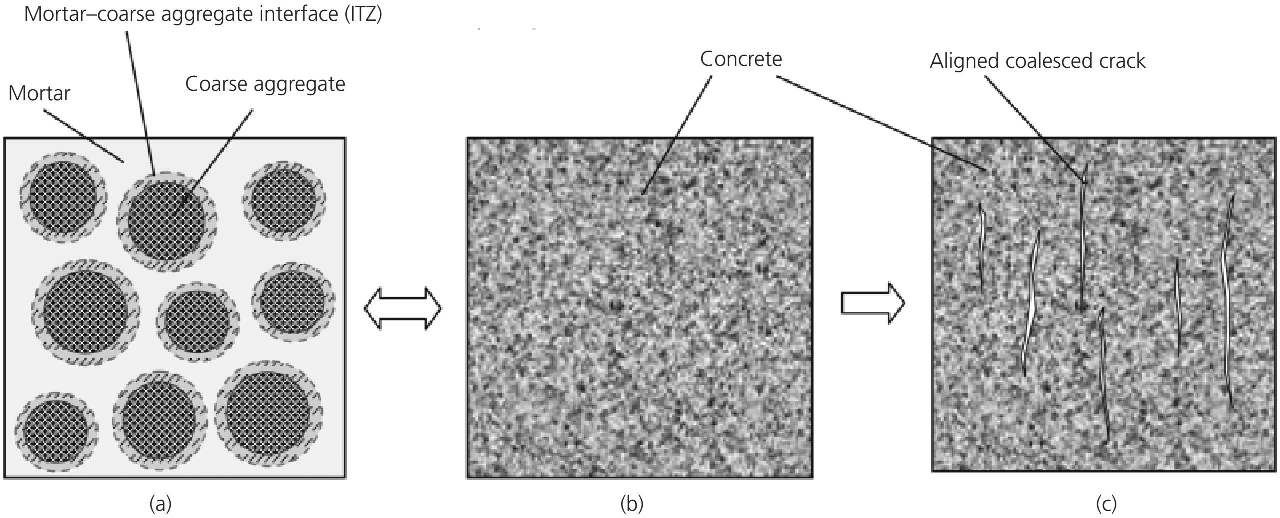

Figure 2. Modelling of concrete: (a) two-phase composite with imperfect interface; (b) concrete; (c) concrete with aligned coalesced cracks

$$\boldsymbol{\varepsilon}^0 = \boldsymbol{L}_0^{-1}\boldsymbol{\sigma}^0 \tag{2}$$

With the inclusion, the stresses and strains in mortar differ from $\boldsymbol{\sigma}^0$ and $\boldsymbol{\varepsilon}^0$ by $\tilde{\boldsymbol{\sigma}}$ and $\tilde{\boldsymbol{\varepsilon}}$, where $\tilde{\boldsymbol{\varepsilon}}$ represents the perturbed strains due to the presence of all the coarse aggregates, and $\tilde{\boldsymbol{\sigma}}$ represents the perturbed stresses. The average stresses in the mortar are then

$$\boldsymbol{\sigma}^{(0)} = \boldsymbol{\sigma}^0 + \tilde{\boldsymbol{\sigma}} = \boldsymbol{L}_0(\boldsymbol{\varepsilon}^0 + \tilde{\boldsymbol{\varepsilon}}) \tag{3}$$

The stresses and strains of the coarse aggregates experience further perturbations from those of the surrounding mortar by $\boldsymbol{\sigma}^{\mathrm{pt}}$ and $\boldsymbol{\varepsilon}^{\mathrm{pt}}$. The average stresses in the aggregate are

$$\begin{aligned}\boldsymbol{\sigma}^{(1)} &= \boldsymbol{\sigma}^0 + \tilde{\boldsymbol{\sigma}} + \boldsymbol{\sigma}^{\mathrm{pt}} \\ &= \boldsymbol{L}_1(\boldsymbol{\varepsilon}^0 + \tilde{\boldsymbol{\varepsilon}} + \boldsymbol{\varepsilon}^{\mathrm{pt}}) \\ &\equiv \boldsymbol{L}_0(\boldsymbol{\varepsilon}^0 + \tilde{\boldsymbol{\varepsilon}} + \boldsymbol{\varepsilon}^{\mathrm{pt}} - \boldsymbol{\varepsilon}^*)\end{aligned} \tag{4}$$

where $\boldsymbol{\varepsilon}^*$ denotes the equivalent transformation strains.

It is assumed that the two sides of the interface are connected to the mortar and the coarse aggregates, respectively. Hence, the interfacial traction remains continuous, while both the normal and the tangential displacements might experience a jump across the interface (Qu, 1993). The interface conditions are given as

$$[\sigma_{ij}]n_j = 0 \tag{5}$$

$$[u_i](\delta_{ik} - n_i n_k) = \alpha_{\mathrm{T}} T_k \tag{6}$$

$$[u_i]\, n_i n_k = \alpha_{\mathrm{N}} N_k \tag{7}$$

in which $\alpha_{\mathrm{T}} > 0$ and $\alpha_{\mathrm{N}} > 0$ denote the compliance in the tangential and the normal directions, respectively; [.] = (out)–(in); n_i is the outward unit normal on the interface; $T_i = \sigma_{kj} n_j(\delta_{ik} - n_i n_k)$ and $N_i = \sigma_{kj} n_k n_j n_i$ represent the shear and the normal tractions, respectively; and δ_{ij} is the Kronecker delta.

For the coarse aggregates with imperfect interface, the relationship between the eigenstrains and the perturbation strains in coarse aggregates is

$$\varepsilon_{ij}^{\mathrm{pt}} = S_{ijkl}\varepsilon_{kl}^* \tag{8}$$

where

$$S_{ijkl} = S_{ijkl}^{\mathrm{E}} + S_{ijkl}^{\mathrm{S}} \tag{9}$$

in which S_{ijkl}^{E} is Eshelby's solution (Eshelby, 1957) for uniform eigenstrain problem of inclusions with perfectly bonded interface and S_{ijkl}^{S} is the additional part considering the elastic spring layer. For the spherical inclusions, the Eshelby's solution S_{ijkl}^{E} is

$$S_{ijkl}^{\mathrm{E}} = \frac{1}{2}\beta^{\mathrm{E}}(\delta_{ik}\delta_{jl} + \delta_{il}\delta_{jk}) + \frac{1}{3}(\alpha^{\mathrm{E}} - \beta^{\mathrm{E}})\delta_{ij}\delta_{kl} \tag{10}$$

with

11. $$\alpha^{\mathrm{E}} = \frac{1+\upsilon_0}{3(1-\upsilon_0)}, \qquad \beta^{\mathrm{E}} = \frac{2(4-5\upsilon_0)}{15(1-\upsilon_0)}$$

where υ_0 is the Poisson ratio of the mortar matrix.

To determine S^{S}_{ijkl} in Equation 9, Zhong and Meguid (1996) considered an infinite medium D containing uniform eigenstrains ε^*_{ij} in a spherical inclusion Ω with an imperfectly bonded interface $\partial\Omega$. The problem is modelled as an equivalent Somigliana dislocation field, and S^{S}_{ijkl} is then defined as

12. $$\left\langle \varepsilon^{\mathrm{S}}_{ij} \right\rangle = S^{\mathrm{S}}_{ijkl}\varepsilon^*_{kl}$$

where

13. $$\varepsilon^{\mathrm{S}}_{ij} = \frac{1}{2}(u^{\mathrm{S}}_{i,j} + u^{\mathrm{S}}_{j,i})$$

Here u^{S}_i denotes the displacement fields caused by the interfacial sliding and normal separation, $\langle \varepsilon^{\mathrm{S}}_{ij} \rangle$ is the body average of $\varepsilon^{\mathrm{S}}_{ij}$ inside the spherical inclusion, that is

14. $$\left\langle \varepsilon^{\mathrm{S}}_{ij} \right\rangle = \frac{1}{\Omega}\int_{\Omega} \varepsilon^{\mathrm{S}}_{ij}\mathrm{d}\Omega$$

If $\varepsilon^{\mathrm{S}}_{ij}$ is separated into its hydrostatic ($\varepsilon^{\mathrm{S}}_{kk}$) and deviatoric ($e^{\mathrm{S}}_{ij}$) components, Equation 12 can be rewritten as

15. $$\left.\begin{aligned} \left\langle \varepsilon^{\mathrm{S}}_{kk} \right\rangle &= \alpha^{\mathrm{S}}\varepsilon^*_{kk} \\ \left\langle e^{\mathrm{S}}_{ij} \right\rangle &= \beta^{\mathrm{S}} e^*_{ij} \end{aligned}\right\}$$

in which

16. $$\alpha^{\mathrm{S}} = \frac{2(1-2\upsilon_0)}{1-\upsilon_0}\lambda_0, \qquad \beta^{\mathrm{S}} = \frac{(7-5\upsilon_0)(5A_0+2B_0)}{75(1-\upsilon_0)}$$

where λ_0, A_0 and B_0 are (Li, 2001)

17a. $$\lambda_0 = \frac{\beta_0 k_1}{3(1+\beta_0 k_1)}$$

17b. $$A_0 = \frac{\alpha_0 k_2 + \alpha_0\beta_0 k_2(k_3+k_4)}{1+\alpha_0(k_2+k_3)+\beta_0 k_4 + \alpha_0\beta_0 k_2(k_3+k_4)}$$

17c. $$B_0 = \frac{(\beta_0-\alpha_0)k_2}{1+\alpha_0(k_2+k_3)+\beta_0 k_4 + \alpha_0\beta_0 k_2(k_3+k_4)}$$

with

$$\alpha_0 = \frac{\mu_0\alpha_{\mathrm{T}}}{a}, \qquad \beta_0 = \frac{\mu_0\alpha_{\mathrm{N}}}{a}$$
$$k_1 = \frac{4(1+\upsilon_0)}{3(1-\upsilon_0)}, \qquad k_2 = \frac{2(7-5\upsilon_0)}{15(1-\upsilon_0)}$$
$$k_3 = \frac{4(7+19\upsilon_0)}{105(1-\upsilon_0)}$$

and

$$k_4 = \frac{4(35+11\upsilon_0)}{105(1-\upsilon_0)}$$

Hence, according to Equations 8–17, the relationship between the eigenstrains and the perturbation strains in the spherical coarse aggregates with imperfect interface are

18. $$\left.\begin{aligned} \varepsilon^{\mathrm{pt}}_{kk} &= (\alpha^{\mathrm{E}}+\alpha^{\mathrm{S}})\,\varepsilon^*_{kk} \equiv \alpha\varepsilon^*_{kk} \\ e^{\mathrm{pt}}_{ij} &= (\beta^{\mathrm{E}}+\beta^{\mathrm{S}})\,e^*_{ij} \equiv \beta e^*_{ij} \end{aligned}\right\}$$

If $\bar{\boldsymbol{\sigma}}$ denotes the overall average stress tensor, then

19. $$\bar{\boldsymbol{\sigma}} = c_0\boldsymbol{\sigma}^{(0)} + c_1\boldsymbol{\sigma}^{(1)} \equiv \boldsymbol{\sigma}^0$$

where c_1 and c_2 represent the volume fractions of mortar and aggregate, respectively; $\boldsymbol{\sigma}^{(0)}$ and $\boldsymbol{\sigma}^{(1)}$ are the stresses in mortar and aggregate, respectively. Substituting Equations 3, 4 and 8 into Equation 19, the perturbation strains in mortar, $\tilde{\boldsymbol{\varepsilon}}$ can be solved as

20. $$\tilde{\boldsymbol{\varepsilon}} = -c_1(\boldsymbol{S}-\boldsymbol{I})\boldsymbol{\varepsilon}^*$$

where the transformation strains $\boldsymbol{\varepsilon}^*$ can thus be solved from Equations 2, 4 and 20 as

21. $$\boldsymbol{\varepsilon}^* = \left[\boldsymbol{L}_0 + (\boldsymbol{L}_1-\boldsymbol{L}_0)(c_0\boldsymbol{S}+c_1\boldsymbol{I})\right]^{-1}(\boldsymbol{L}_0-\boldsymbol{L}_1)$$

Substituting Equations 20 and 21 into Equations 3 and 4, the average stresses in the mortar (with superscript 0) and the coarse aggregates (with superscript 1) are

$$\sigma^{(0)} = \frac{\kappa_0 + \alpha(\kappa_1 - \kappa_0)}{\kappa_0 + (c_1 + c_0\alpha)(\kappa_1 - \kappa_0)}\bar{\sigma} \tag{22a}$$

$$\boldsymbol{s}^{(0)} = \frac{\mu_0 + \beta(\mu_1 - \mu_0)}{\mu_0 + (c_1 + c_0\beta)(\mu_1 - \mu_0)}\bar{\boldsymbol{s}} \tag{22b}$$

$$\sigma^{(1)} = \frac{\kappa_1}{\kappa_0 + (c_1 + c_0\alpha)(\kappa_1 - \kappa_0)}\bar{\sigma} \tag{23a}$$

$$\boldsymbol{s}^{(1)} = \frac{\mu_1}{\mu_0 + (c_1 + c_0\beta)(\mu_1 - \mu_0)}\bar{\boldsymbol{s}} \tag{23b}$$

where κ_i denotes the bulk moduli of mortar ($i = 0$) or coarse aggregates ($i = 1$) and μ_i represents the shear moduli of mortar ($i = 0$) or coarse aggregates ($i = 1$). If there is no special statement below, the hydrostatic and deviatoric components of the stress and strain tensors will be written as σ and $\boldsymbol{s}$, ε and $\boldsymbol{e}$, respectively.

The strains in the mortar and the coarse aggregates are

$$\varepsilon^{(0)} = \frac{\boldsymbol{\sigma}^{(0)}}{\kappa_0} = \frac{\kappa_0 + \alpha(\kappa_1 - \kappa_0)}{\kappa_0 + (c_1 + c_0\alpha)(\kappa_1 - \kappa_0)}\varepsilon^0 \tag{24a}$$

$$\boldsymbol{e}^{(0)} = \frac{\boldsymbol{s}^{(0)}}{2\mu_0} = \frac{\mu_0 + \beta(\mu_1 - \mu_0)}{\mu_0 + (c_1 + c_0\beta)(\mu_1 - \mu_0)}\boldsymbol{e}^0 \tag{24b}$$

$$\varepsilon^{(1)} = \frac{\boldsymbol{\sigma}^{(1)}}{\kappa_1} = \frac{\kappa_0}{\kappa_0 + (c_1 + c_0\alpha)(\kappa_1 - \kappa_0)}\varepsilon^0 \tag{25a}$$

$$\boldsymbol{e}^{(1)} = \frac{\boldsymbol{s}^{(1)}}{2\mu_1} = \frac{\mu_0}{\mu_0 + (c_1 + c_0\beta)(\mu_1 - \mu_0)}\boldsymbol{e}^0 \tag{25b}$$

The body average of the strains can be defined as (Benveniste, 1985)

$$\bar{\varepsilon}_{ij} = c_0\varepsilon_{ij}^{(0)} + c_1\varepsilon_{ij}^{(1)} + \frac{1}{2V}\int_S ([u_i]\,n_j + [u_j]\,n_i)\,\mathrm{d}\boldsymbol{S} \tag{26}$$

in which V is the volume of whole body; $[u_i]$ can be written as (Zhong and Meguid, 1996)

$$[u_i] = -\lambda_0\varepsilon_{ll}^* x_i - A_0 e_{ij}^* x_j - \frac{1}{a^2}B_0 e_{kl}^* x_k x_l x_i \tag{27}$$

where a is the average radius of the coarse aggregates.

Substituting Equations 24, 25 and 27 into Equation 26, gives

$$\bar{\varepsilon} = \frac{\kappa_0 + (c_0\alpha + c_1\lambda_0)(\kappa_1 - \kappa_0)}{\kappa_0 + (c_1 + c_0\alpha)(\kappa_1 - \kappa_0)}\varepsilon^0 \tag{28a}$$

$$\bar{\boldsymbol{e}} = \frac{\mu_0 + (c_1 A_0 + c_0\beta)(\mu_1 - \mu_0)}{\mu_0 + (c_1 + c_0\beta)(\mu_1 - \mu_0)}\boldsymbol{e}^0 \tag{28b}$$

The equivalent bulk and shear moduli of the concrete can be obtained from

$$\frac{\kappa}{\kappa_0} = \frac{\kappa_0 + (c_1 + c_0\alpha)(\kappa_1 - \kappa_0)}{\kappa_0 + (c_1\lambda_0 + c_0\alpha)(\kappa_1 - \kappa_0)} \tag{29a}$$

$$\frac{\mu}{\mu_0} = \frac{\mu_0 + (c_1 + c_0\beta)(\mu_1 - \mu_0)}{\mu_0 + (c_1 A_0 + c_0\beta)(\mu_1 - \mu_0)} \tag{29b}$$

Fraction of failed interfaces

Lambrigger (1997) pointed out that Weibull distribution function (Weibull, 1951) could correctly characterise the strength and failure of macroscopically homogeneous specimens. The Weibull distribution function has been applied in the field of damage mechanics and concrete failure analysis (Chen, 1995; Karihaloo, 1995; Yip *et al.*, 1995). In this research, it is again adopted to evaluate the fraction of failed interfaces.

It is assumed that the fraction of failed interfaces between mortar and coarse aggregates conforms to a Weibull distribution function as

$$c_i(\varepsilon) = 1 - \exp\left[-\left(\frac{\varepsilon}{\varepsilon_{u1}}\right)^{m_1}\right] \tag{30}$$

where c_i is the fraction of failed interfaces and ε is the effective strain of concrete. In the case of uniaxial compression, $\varepsilon = \varepsilon_3$ and the subscript '3' represents the compressive stress direction. ε_{u1} is the ultimate strain. If c_i is set to be 1 when ε equals ε_{u1}, Equation 30 can be normalised as

$$c_i(\varepsilon) = \frac{1}{1 - e^{-1}}\left\{1 - \exp\left[-\left(\frac{\varepsilon}{\varepsilon_{u1}}\right)^{m_1}\right]\right\} \quad (31)$$

Hence, the equivalent bulk and shear moduli of concrete with the fraction of failed interfaces c_i are

$$\kappa_e = c_i\kappa_d + (1 - c_i)\kappa_p, \qquad \mu_e = c_i\mu_d + (1 - c_i)\mu_p \quad (32)$$

where κ_d and μ_d are the bulk and shear moduli of concrete with destroyed interfaces. They can be calculated from Equations 29, 16, 17 and 11 with the interface parameters in Equation 17, $\alpha_0 = \infty$ and $\beta_0 = \infty$. κ_p and μ_p in Equation 32 are the bulk and shear moduli of concrete with perfect interfaces, which can also be calculated from Equations 29, 16, 17 and 11, but with the interface parameters $\alpha_0 = 0$, $\beta_0 = 0$. Owing to the isotropy of concrete, if κ_e and μ_e are known, the Young's modulus E_e and the Poisson ratio υ_e of the concrete with imperfect interfaces are

$$E_e = \frac{9\kappa_e\mu_e}{3\kappa_e + \mu_e}, \qquad \upsilon_e = \frac{3\kappa_e - 2\mu_e}{6\kappa_e + 2\mu_e} \quad (33)$$

Equivalent moduli of concrete with aligned coalesced cracks

With further increase of load, the microcracks in the mortar–coarse aggregate ITZ will propagate into mortar and aggregates and coalesce to finally cause the failure of the concrete. These coalesced cracks are considered as a series of aligned cracks caused by the principal tensile strain. These aligned coalesced cracks should be perpendicular to the direction of the principal tension strain and they are considered as voids, a kind of material whose moduli are zeros. According to the Mori–Tanaka method (Benveniste, 1987; Mori and Tanaka, 1973), the overall moduli of two-phase composite can be solved as

$$\boldsymbol{L} = \boldsymbol{L}_e + c_v[(\boldsymbol{L}_v - \boldsymbol{L}_e)\boldsymbol{T}][(1 - c_v)\boldsymbol{I} + c_v\boldsymbol{T}]^{-1} \quad (34a)$$

with

$$\boldsymbol{T} = \{\boldsymbol{I} + [(1 - c_v)\boldsymbol{S} + c_v\boldsymbol{I}]\,\boldsymbol{L}_e^{-1}(\boldsymbol{L}_v - \boldsymbol{L}_e)\}^{-1} \quad (34b)$$

where subscript 'e' represents concrete (mortar + aggregates + interfaces) and subscript 'v' represents voids with $\boldsymbol{L}_v \equiv 0$. c_v is the volume ratio of aligned cracks to overall concrete volume. If there is a series of aligned inclusions in a certain composite (Figure 2(c)), the corresponding Eshelby's tensor $\boldsymbol{S}$ can be given as (Mura, 1987)

$$\boldsymbol{S} = \begin{bmatrix} 0 & 0 & 0 & 0 & 0 & 0 \\ \frac{\upsilon_e}{2(1-2\upsilon_e)} & \frac{5-4\upsilon_e}{8(1-\upsilon_e)} & \frac{4\upsilon_e-1}{8(1-\upsilon_e)} & 0 & 0 & 0 \\ \frac{\upsilon_e}{2(1-2\upsilon_e)} & \frac{4\upsilon_e-1}{8(1-\upsilon_e)} & \frac{5-4\upsilon_e}{8(1-\upsilon_e)} & 0 & 0 & 0 \\ 0 & 0 & 0 & \frac{3-4\upsilon_e}{8(1-\upsilon_e)} & 0 & 0 \\ 0 & 0 & 0 & 0 & \frac{1}{4} & 0 \\ 0 & 0 & 0 & 0 & 0 & \frac{1}{4} \end{bmatrix} \quad (35)$$

where the Poisson ratio of the concrete with imperfect interfaces υ_e is given in Equation 33. For the plane stress problem (Figure 3), Equation 35 can be expressed as

$$\boldsymbol{S} = \begin{bmatrix} 0 & 0 & 0 \\ \frac{\upsilon_e}{2(1-\upsilon_e)} & \frac{5-4\upsilon_e}{8(1-\upsilon_e)} & 0 \\ 0 & 0 & 1/2 \end{bmatrix} \quad (36)$$

The Weibull distribution has been used again to model the evolution of the volume ratio of the aligned coalesced cracks in the material. The failure volume ratio under the current principal tensile strain is therefore

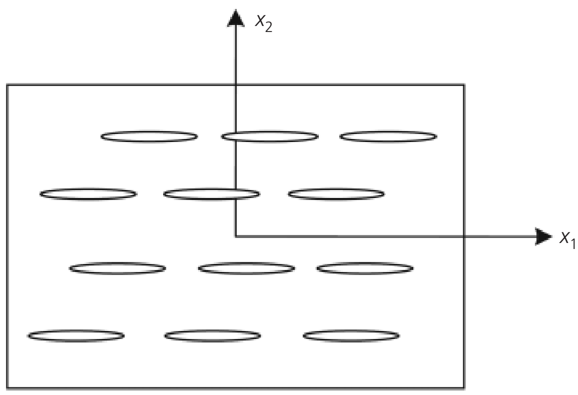

Figure 3. Concrete with aligned coalesced cracks (two dimensional)

37. $$c_{\mathrm{v}}(\varepsilon_1) = \frac{1}{1-\mathrm{e}^{-1}}\left\{1-\exp\left[-\left(\frac{\varepsilon_1}{\varepsilon_{\mathrm{u}2}}\right)^{m_2}\right]\right\}$$

where ε_1 is the first principal tensile strain in mortar, $\varepsilon_{\mathrm{u}2}$ is the ultimate tensile strain value (when ε_1 reaches the value of $\varepsilon_{\mathrm{u}2}$, the mortar fails completely), and m_2 is a shape index. When the principal tension reaches the critical value for cracking, Equation 37 can be used to obtain the current volume ratio of aligned cracks. The moduli of concrete are calculated from Equations 34–36. The flowchart implementing this model is shown in Figure 4.

Model parameters

The main parameters include the shape indexes m_1, m_2 and the threshold values of strain $\varepsilon_{\mathrm{u}1}$, $\varepsilon_{\mathrm{u}2}$. These parameters usually cannot be measured directly. Based on simulation for concrete, m_1 and $\varepsilon_{\mathrm{u}1}$, which is related to the interface failure and compression of concrete, are set to 3 and 0·008, respectively. m_2 and $\varepsilon_{\mathrm{u}2}$ are related to the tensile strain induced mortar failure in the concrete. Here $\varepsilon_{\mathrm{u}2}$ is defined as (Bazant *et al.*, 1990; Mohamed and Hansen, 1999)

38. $$\varepsilon_{\mathrm{u}2} = \frac{2G_{\mathrm{F}}}{f_{\mathrm{t}} l_{\mathrm{m}}}$$

where f_{t} is the tensile strength for concrete, G_{F} is the fracture energy of concrete and l_{m} is the eigen-length for mortar. According to the CEB-FIP code (CEB-FIP, 1993), there is a simple empirical formula relating G_{F} $(\mathrm{J/m^2} \equiv \mathrm{N/m})$ to the compressive strength f'_{c} (MPa), as $G_{\mathrm{F}} = \alpha_{\mathrm{F}}(f'_{\mathrm{c}})^{0{\cdot}7}$, where the empirical coefficient α_{F} depends on the maximum aggregate size g (Table 1). The tensile strength f_{t} can be calculated from empirical equations suggested by ACI Committee 209

Maximum aggregate size g: mm	α_{F}
8	4
16	6
32	10

Table 1. Coefficient α_{F} with maximum aggregate size g (Karihaloo, 1995)

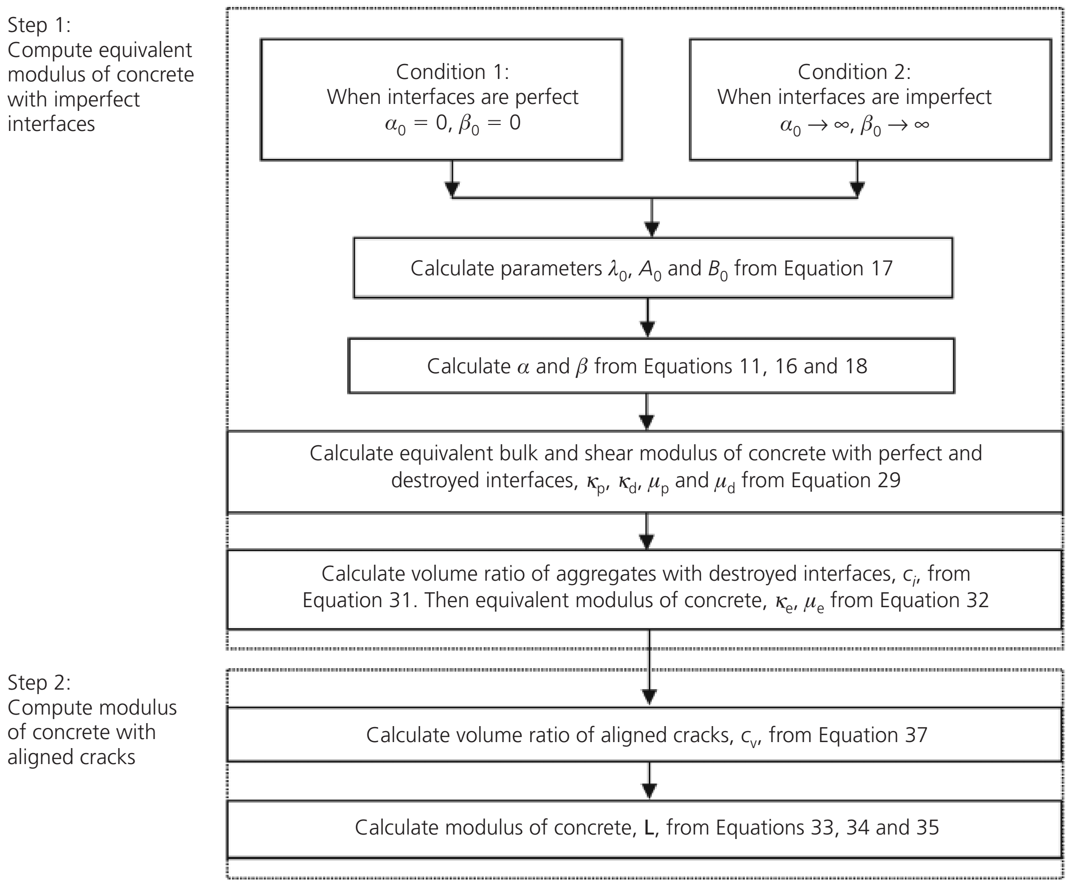

Figure 4. Outline for calculation of concrete modulus

39a. $f_t = \frac{1}{3}(wf'_c)^{1/2}$ psi (w in pcf and f'_c in psi)

39b. $f_t = 0{\cdot}2187(wf'_c)^{1/2}$ kPa (w in kg/m^3 and f'_c in kPa)

where w is the density of concrete. For normal weight concrete, Equation 39b can be rewritten as (in MPa)

40. $f_t = 1{\cdot}59 f_c'^{1/2}$

According to Bazant's random particle model, $l_m = \beta_F g$ and β_F is roughly considered to be 1/2. Thus Equation 38 becomes

41. $\varepsilon_{u2} = 2{\cdot}5143 f_c'^{0{\cdot}2} \frac{\alpha_F}{g}$

The suitable value of m_2 is found here to be

42. $m_2 = 8{\cdot}4 - 7{\cdot}55 \exp(-0{\cdot}1\rho^{3{\cdot}57})$

where $\rho = \varepsilon_{u2}/\varepsilon_r$ and $\varepsilon_r = 3{\cdot}34 - 1{\cdot}59 \exp(-3{\cdot}1 \times 10^5 \varepsilon_{u2}^{-20{\cdot}48})$. The parametric studies show that m_2 is related to the strength of mortar. The higher the strength of mortar, the larger the value of m_2. ε_{u2} is related to the ductility properties of concrete. The lower the strength of mortar/concrete, the better the ductility properties of concrete/mortar and so the larger is ε_{u2}.

The proposed model needs the volume ratio of mortar (c_0) and concrete (c_1), and their bulk and shear moduli (κ_0, μ_0, κ_1 and μ_1), as inputs. In applications, their densities (ρ_0, ρ_1 and w), initial elastic moduli (E_0 and E_1), and Poisson ratios (υ_0 and υ_1) can be used to calculate the inputs as shown in the next section. The evolution rule of the fraction of failed interfaces (c_i) is fixed. To describe the evolution of the volume ratio of the aligned coalesced cracks (c_v), the diameter of aggregates (g) and the compressive strength (f'_c) are needed. A lower compressive strength or a larger size of aggregates leads to a slower development of aligned coalesced cracks and better ductility properties of the concrete/mortar.

Numerical examples

It is worth noting that the lateral deformation increases significantly at higher stress level near the peak load where large cracks appear and crack growth becomes unstable. To properly describe the lateral strain during the descending branch, the following equation is used to modify the change in lateral strain after the peak load under uniaxial compression.

43. $\bar{\varepsilon}_{\text{lateral}} = 200e^{-e^{1{\cdot}667-5\lambda_l}} \varepsilon_{\text{lateral}}$

where

44. $\lambda_l = 1 - \sigma_{\text{compression}}/f'_c$

Zhang (2001) had tested the behaviours of concrete and mortar. The mortar and concrete were pan mixed in the laboratory and were cast in steel moulds (100 mm in diameter and 200 mm high). The mix design is shown in Table 2. Mortar G40 includes no coarse aggregate; GC40 and GC50 are normal concrete with different contents of coarse aggregate.

The densities of the mortar ρ_0, coarse aggregate ρ_1 and concrete w can be measured. The volume fraction of the mortar (c_0) and coarse aggregate ($c_1 = 1 - c_0$) can thus be calculated from

45. $w = c_0\rho_0 + (1 - c_0)\rho_1$

Uniaxial compression tests were then performed to obtain the initial elastic moduli and Poisson ratios of mortar (E_0, υ_0) and concrete (E_e, υ_e). From Equation 32, the bulk and shear moduli of concrete are

46. $\kappa_e = \frac{E_e}{3(1 - 2\upsilon_e)} = \kappa_p, \quad \mu_e = \frac{E_e}{2(1 + \upsilon_e)} = \mu_p$

The bulk and shear moduli of mortar are similarly

47. $\kappa_0 = \frac{E_0}{3(1 - 2\upsilon_0)}, \quad \mu_0 = \frac{E_0}{2(1 + \upsilon_0)}$

The bulk and shear moduli of the coarse aggregate, κ_1 and μ_1, can be solved from Equation 29 and the initial elastic moduli and Poisson ratios of the coarse aggregate can be obtained similarly to Equation 33. The properties of mortar and concrete are shown in Table 3 and Table 4, respectively.

In Figure 5, it is shown that the proposed model can predict the

Grade	Cement	Sand	Water	Coarse aggregate
G40 mortar	1	2·8	0·35	None
GC40 concrete	1	2·8	0·35	2·8
GC50 concrete	1	2·8	0·35	1·4

Table 2. Mix design of specific weight ratio for mortar and concrete (Zhang, 2001)

Initial modulus: GPa	Compressive strength: MPa	ε_{u2}	m_2
25·3	37·74	0·0016	1·51

Note: ε_{u2} is calculated from Equation 41; m_2 is from Equation 42.

Table 3. Elastic properties of G40 mortar (Zhang, 2001)

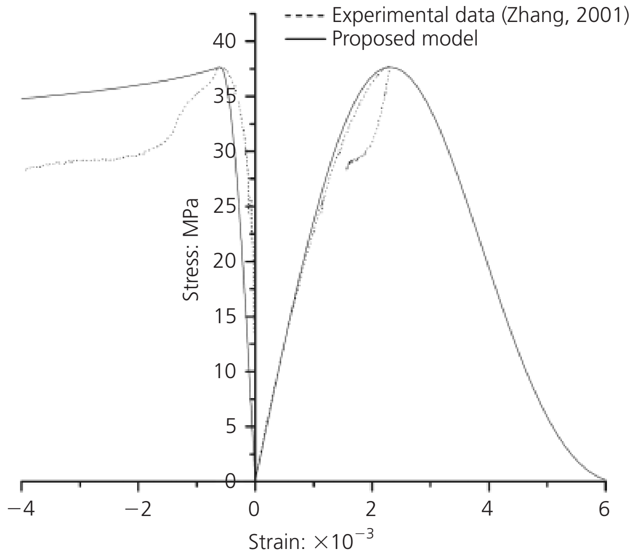

Figure 5. Stress–strain curve for mortar

mortar behaviour reasonably well, especially for the ascending part and the peak load. It is also shown that the aligned coalesced crack model can properly evaluate the failure of mortar.

The proposed model is further used to predict the compressive behaviour of the concrete. The predicted responses of the compressive behaviour including the lateral strains are shown in Figures 6–11 to be reasonably good.

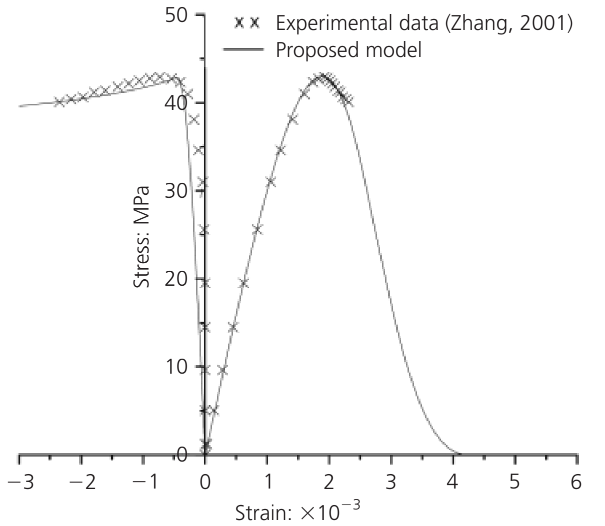

Figure 6. Stress–strain relation of concrete GC40-1

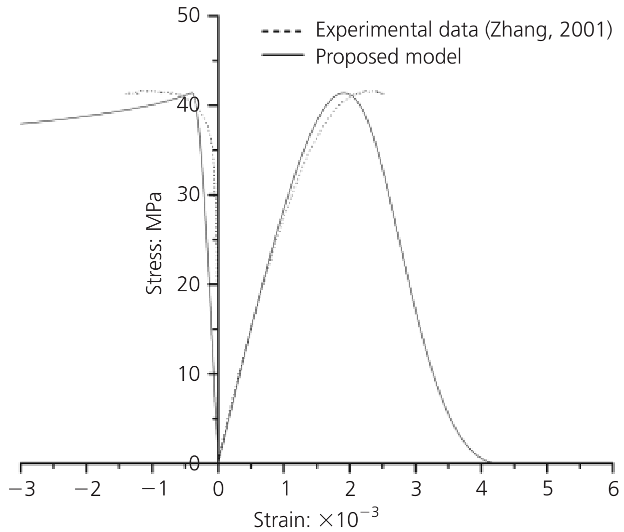

Figure 7. Stress–strain relation of concrete GC40-2

Grade	Density of mortar (assumed): kg/m^3	Density of coarse aggregates (assumed): kg/m^3	Volume ratio of mortar	Elastic modulus of concrete: GPa	Elastic modulus of coarse aggregates: GPa
GC40-1	2400	2640	0·6198	32·69	50·69
GC40-2	2400	2640	0·6198	30·78	42·70
GC40-3	2400	2640	0·6198	30·25	40·69
GC50-1	2400	2640	0·7653	31·02	63·41
GC50-2	2400	2640	0·7653	31·06	63·83
GC50-3	2400	2640	0·7653	31·31	66·57

Table 4. Properties of concrete (Zhang, 2001)

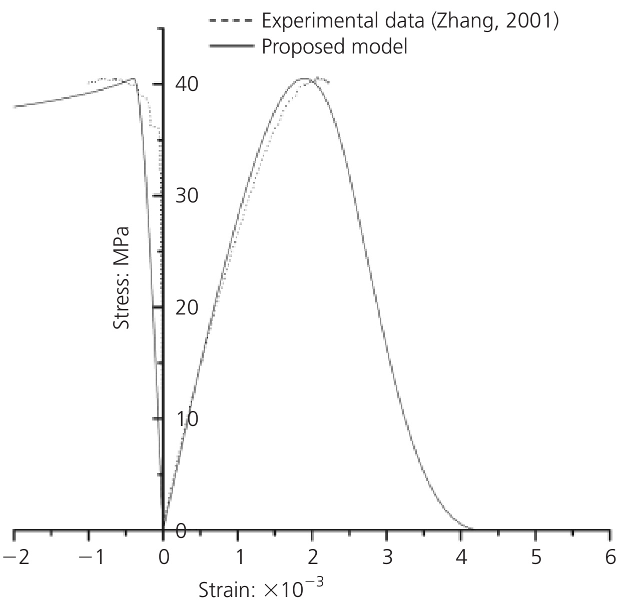

Figure 8. Stress–strain relation of concrete GC40-3

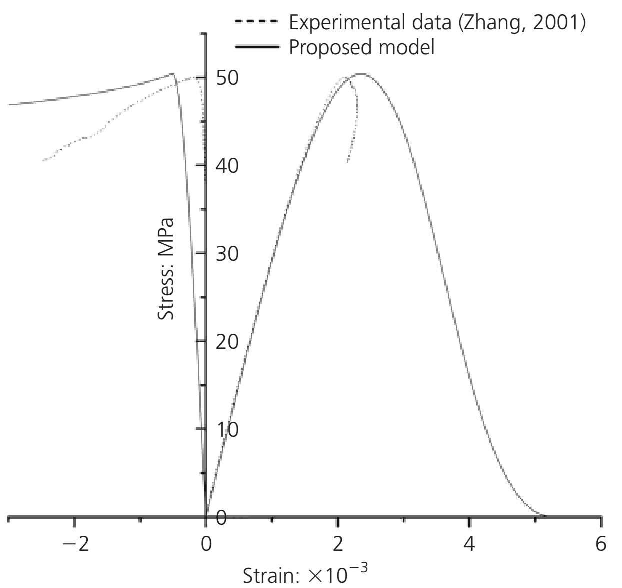

Figure 9. Stress–strain relation of concrete GC50-1

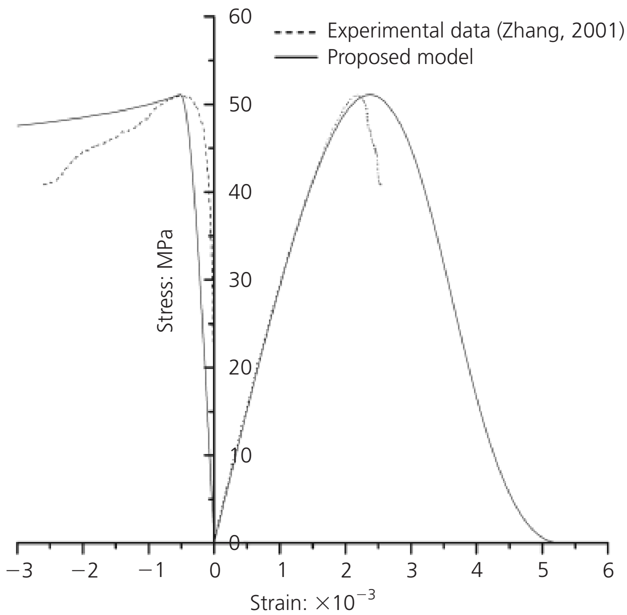

Figure 10. Stress–strain relation of concrete GC50-2

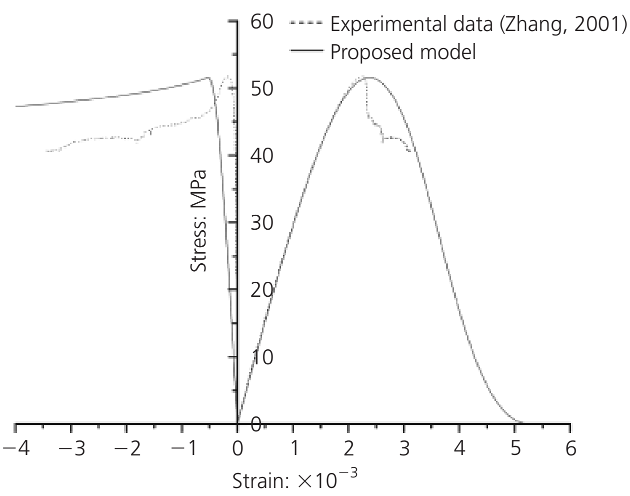

Figure 11. Stress–strain relation of concrete GC50-3

In order to explore the capability of the model in predicting the transition in behaviour from low- to high-strength concrete, two more examples are studied (Dahl, 1992; Neville, 1995). The experimental data for concrete with different strength levels are listed in Tables 5 and 6. In comparison with those obtained experimentally, these predictions are reasonably accurate as shown in the Figures 12 and 13.

Conclusions

In this paper, a micromechanical model based on the Mori–Tanaka method is developed to study the stress–strain behaviour of concrete under uniaxial compression. The concrete is modelled as a two-phase composite with an imperfect bond between mortar and coarse aggregate. The aligned coalesced cracks are then considered as void inclusions in the matrix of the concrete. The Weibull distribution function is used to describe the developments of the two kinds of defects in the material.

The proposed model has been used to study the stress–strain

f'_c: MPa	E_e: GPa	E_0: GPa	m_2	ε_{u2}: $\times 10^{-3}$	$\varepsilon_r \times 10^{-3}$
20·8329	20·23	12·6347	0·9	1·7307	3·3
28·6999	24·66	16·6408	1·0	1·8452	2·9
35·7387	28·28	20·3116	1·25	1·9279	2·3
42·3858	30·34	21·2075	1·6	1·9948	2·0
55·8684	34·13	27·0243	1·8	2·1081	1·9
69·7838	37·53	31·3671	2·1	2·2040	1·8
83·6917	38·98	33·3155	2·5	2·2856	1·8

Note: ε_{u2} is calculated from Equation 41; m_2 and ε_r are from Equation 42.

Table 5. Material properties and coefficients for the proposed model (Neville, 1995)

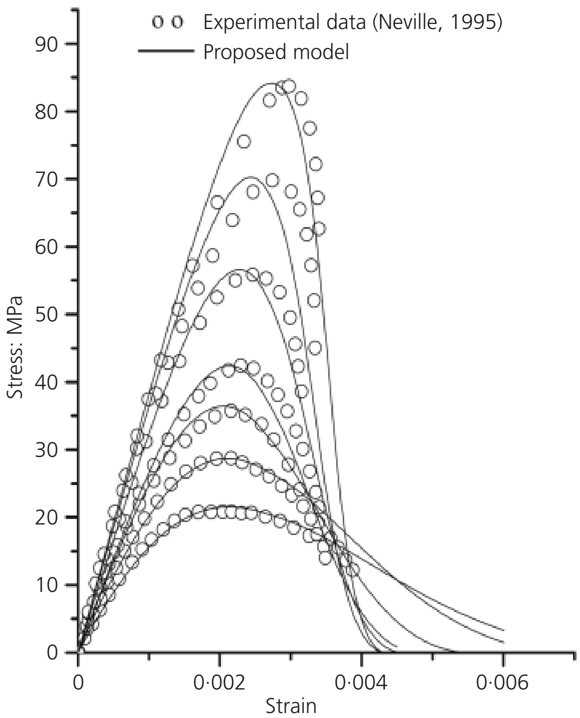

Figure 12. Stress–strain curves of different strength for concrete (Neville, 1995)

relationships of mortar and concrete. The results obtained conform to the experimental data, which show that the proposed micromechanical model is capable of predicting the entire response of concrete under uniaxial compression and is worthy of further research and development.

The failure mechanism assumed in this paper is also verified. The failure of the mortar–coarse aggregate interfaces (ITZs) is described by the increase of the fraction of failed interface (c_i) which is a function of compressive strain (Equation 31). The

f'_c: MPa	E_e: GPa	E_0: GPa	m_2	ε_{u2}: $\times 10^{-3}$	$\varepsilon_r \times 10^{-3}$
105·80	42·85	38·786	2·815	2·395	1·758
94·17	40·00	34·720	2·663	2·340	1·763
67·40	33·30	26·013	2·219	2·189	1·802
50·30	30·00	22·195	1·772	2·064	1·917
31·70	26·60	18·563	1·092	1·882	2·578
22·00	20·00	12·441	0·930	1·750	3·280

Note: ε_{u2} is calculated from Equation 41; m_2 and ε_r are from Equation 42.

Table 6. Material properties and coefficients for the proposed model (Dahl, 1992)

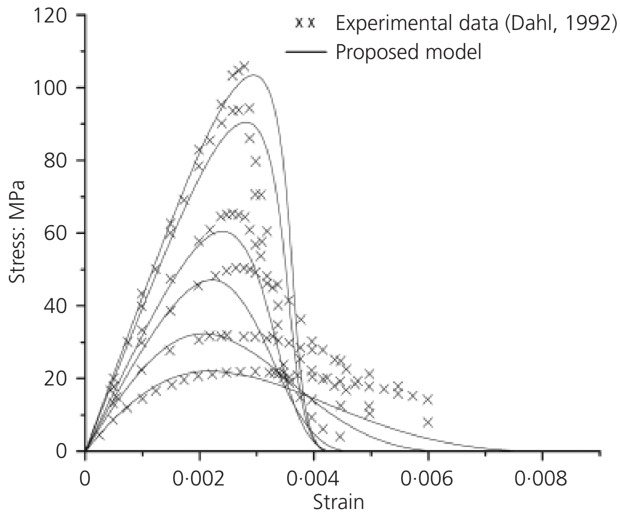

Figure 13. Stress–strain curves of different strength for concrete (Dahl, 1992)

development of the aligned coalesced crack in the concrete is quantified by its volume ratio (c_v), which is a function of tensile strain (Equation 37). The Weibull distribution function has been shown to be able to describe the development of the cracks in the concrete and in the interfaces.

Acknowledgements

The authors would like to acknowledge the research fund provided by the National Research Foundation of Singapore (NRF) through the NRF-CRP Research Programme 'Underwater infrastructure and underwater city of the future'.

REFERENCES

Bazant ZP, Tabbara MR, Kazemi MT and Pijaudier-Cabot G (1990) Random particle model for fracture of aggregate or fibre composite. *Journal of Engineering Mechanics* **116(8)**: 1686–1704.

Benveniste Y (1985) The effective mechanical behaviour of composite materials with imperfect contact between the constituents. *Mechanics of Materials* **4(3)**: 197–208.

Benveniste Y (1987) A new approach to the application of Mori–Tanaka's theory in composite materials. *Mechanics of Materials* **6(2)**: 147–157.

CEB-FIP (Comité Euro-International du Béton–Fédération International de la Précontrainte) (1993) *Model Code 1990, 1993*. Thomas Telford, London, UK, MC90.

Chen EP (1995) Dynamic brittle material response based on a continuum damage model. In *Impact Waves and Fracture* (Barta RC, Mal AK and MacSithigh GP (eds)). ASME, (Applied Mechanics Division), Vol. 205, pp. 21–34.

Dahl KKB (1992) *Uniaxial Stress–strain Curves for Normal and High-strength Concrete*. Department of Structural Engineering and Materials, Technical University of Denmark, Lyngby, Demark, Report No. R282.

Eshelby JD (1957) The determination of the field of an ellipsoidal inclusion and related problems. *Proceedings of the Royal Society* **A(241)**: 376–396.

Hashin Z and Monteiro P (2002) An inverse method to determine the elastic properties of the interphase between the aggregate and the cement paste. *Cement and Concrete Research* **32(8)**: 1291–1300.

He H, Stroeven P, Stroeven M and Sluys LJ (2012) Influence of particle packing on elastic properties of concrete. *Magazine of Concrete Research* **64(2)**: 163–175.

Karihaloo BL (1995) *Fracture Mechanics and Structural Concrete*. Longman, London, UK.

Lambrigger M (1997) Alternative scaling of cumulative Weibull failure probability distribution functions. *Journal of Material Science Letters* **16(19)**: 1537–1539.

Li Q (2001) *A Micromechanics-based Constitutive Model and its Application to Lattice Analysis of Plain Concrete*. PhD thesis, Nanyang Technological University, Singapore.

Mohamed AR and Hansen W (1999) Micromechanical modelling of concrete response under static loading – Part 1: Model development and validation. *ACI Materials Journal* **96(2)**: 196–203.

Mori T and Tanaka K (1973) Average stress in the matrix and average elastic energy of materials with mis-fitting inclusions. *Acta Metallurgica* **21(5)**: 571–574.

Mura T (1987) *Micromechanics of Defects in Solids*. Kluwer Academic, Dordrecht, the Netherlands.

Neville AM (1995) *Properties of Concrete*, 4th edn. Longman Scientific & Technical, New York, USA.

Nilsen AU and Monteiro PJM (1993) Concrete: a three phase material. *Cement and Concrete Research* **23(1)**: 147–151.

Qu J (1993) The effect of slightly weakened interfaces on the overall elastic properties of composite materials. *Mechanics of Materials* **14(4)**: 269–281.

Ramesh G, Sotelino ED and Chen WF (1996) Effect of transition zone on elastic moduli of concrete materials. *Cement and Concrete Research* **26(4)**: 611–622.

Ricaud JM and Masson R (2009) Effective properties of linear viscoelastic heterogeneous media: internal variables formulation and extension to ageing behaviours. *International Journal of Solids and Structures* **46(7–8)**: 1599–1606.

Weibull W (1951) A statistical distribution function of wide applicability. *Journal of Applied Mechanics* **18(1)**: 293–297.

Yang CC and Huang R (1996) Double inclusion model for approximate elastic moduli of concrete materials. *Cement and Concrete Research* **26(1)**: 83–91.

Yip WK, Konga FK, Chana KS and Limb MK (1995) A statistical model of microcracking of concrete under uniaxial compression. *Theoretical and Applied Fracture Mechanics* **22(1)**: 17–27.

Zhang JG (2001) *Tri-axial Behaviour of Cement Mortar Under Monotonic Loading*. Masters thesis, Nanyang Technological University, Singapore.

Zheng JJ, Guo ZQ, Pan XD, Stroeven P and Sluys LJ (2011) ITZ volume fraction in concrete with spheroidal aggregate particles and application: Part I. Numerical algorithm. *Magazine of Concrete Research* **63(7)**: 473–482.

Zhong Z and Meguid SA (1996) On the eigenstrain problem of a spherical inclusion with an imperfectly bonded interface. *ASME Journal of Applied Mechanics* **63(4)**: 877–883.